Penetration of Vapor Jets Submerged in Subcooled Liquids

An experimental investigation of the penetration distance required for complete condensation of a submerged turbulent vapor jet injected into a quiescent liquid bath of the same material was made. The bath was maintained in a subcooled condition at a temperature below the boiling temperature of the liquid at the bath pressure. The experiments were limited to choked injector flows with the penetration regime such that buoyancy effects are negligible. Tests were run for water, ethylene glycol, and iso-octane over a range of flow rates and bath pressures. A theoretical expression for the vapor penetration distance was developed utilizing a variable density single fluid model for the two-phase flow, with the turbulent mixing process treated by an entrainment law. Corrections for the external expansion of the choked flow beyond the injector exit were also determined. This model was found to correlate the results of both the present experiments and those of earlier investigators over a wide range of operating conditions and injector geometries.

J. C. WEIMER
G. M. FAETH
and D. R. OLSON

Department of Mechanical Engineering
Pennsylvania State University
University Park, Pennsylvania 16802

SCOPE

The injection of a condensing or reacting gas into a liquid bath occurs in a variety of industrial operations. For example, the condensing jet has been considered for direct contact feedwater heaters, underwater propulsion systems, and for the blowdown of primary nuclear boiler systems into a water bath, without releasing fissionable materials to the atmosphere. Reacting jets are of interest in metal processing and also for thermal energy sources involving submerged injection of an oxidizer into a liquid metal bath. Other applications involve dissolving a gas in a bulk liquid phase.

The present investigation considers the condensing jet problem and relates only by analogy to the other processes mentioned above. In this instance, the vapor jet enters a liquid bath of the same material which is in a subcooled condition at a temperature below the boiling temperature of the liquid at the pressure of the bath. The most distinctive feature of this injection process is that the condensation of the vapor causes the gaseous portion of the flow to extend (penetrate) only a finite distance into the liquid. The penetration length of the vapor is an important factor in system design, since it is ordinarily desirable that condensation be completed within the liquid bath. Therefore, the major objective of the present investigation was to establish a correlation for predicting the vapor penetration length over a wide range of operating conditions.

Past experimental work on this problem by Glikman (1959), Gilbert and Bozic (1966), Stanford and Webster (1972), and Kerney et al. (1972), has been limited to the steam-water system with the bath at atmospheric pressure. Under these conditions, Kerney et al. (1972) developed a correlation for the vapor penetration length (for choked injector flows) which included the effect of injector diameter, flow rate, and bath temperature.

The present investigation extends this earlier work by considering in addition to the steam-water system, the liquid-vapor systems of ethylene glycol and iso-octane. The experiments also employed a liquid bath contained in a closed vessel so that the influence of varying bath pressure could be investigated. As in earlier investigations, tests were conducted over a range of bath temperatures and injector flow rates. The experiments were limited to choked injector flows, however, in order to avoid the complications of oscillatory injector operation described by Kerney et al. (1972). For these high flow rates, there is a broad range of operating conditions where buoyancy effects are negligible and this phenomena was not considered in the present investigation.

A semi-empirical model of the condensing jet process was developed to aid in correlating the data. For the purposes of this model, the flow field was divided into two regions. The region adjacent to the injector exit, where the flow expands to the pressure of the bath, was treated as an isentropic expansion with negligible mixing with the bath liquid. Following external expansion, the condensation process was assumed to be completed by turbulent mixing with the bath liquid. In the mixing region, the two-phase jet was represented by a variable density, single fluid model (Bankoff, 1960). Turbulent mixing was treated by an entrainment model, corrected for the density difference between the jet and the ambient fluid (Morton, 1965).

CONCLUSIONS AND SIGNIFICANCE

Data correlation employed experimental results for choked injector flows from both Kerney et al. (1972) and the present investigation. The vapor penetration length in a quiescent liquid bath is given as

$$x_c/r_0 = 35.5\ (G_0/G_s)^{1/2}/[(\rho_\infty/\rho_s)^{1/2}B]$$

In this equation, the mass velocity ratio results from the

Correspondence concerning this paper should be addressed to G. M. Faeth. J. C. Weimer is with Westinghouse Electric Corporation, Lester, Pennsylvania.

external expansion of the vapor, the density ratio results from the turbulent entrainment law, and B is the driving potential for condensation [defined in Equation (17)].

As illustrated in Figure 3, the above correlation was equally suitable for water, ethylene glycol and iso-octane. For dimensionless penetration lengths in the range 3-70, with the test conditions given in Table 1, the average absolute deviation of this equation was 21.9%. Although of less fundamental singnificance, a multiple regression fit of the data, Equation (22), provides a better numerical prediction of the penetration length (average error 13.0%).

Similar to other turbulent jet processes, the flow was found to be relatively independent of molecular transport properties (as represented by the Prandtl number) and the injector Reynolds number. The constant in the above equation is of the same order of magnitude as the value suggested by the turbulent mixing characteristics of gaseous jets (Ricou and Spalding, 1961; Murgai and Emmons, 1960). This implies that two-phase condensing jets exhibit gross similarities to the mixing characteristics of single-phase jets, when allowance is made for the large density variation of the condensing jet. The application of the above equation, by analogy, to a two-phase reacting or dissolving jet remains to be tested; however, the origin of the terms in the equation suggests this possibility through a proper redefinition of the driving potential B.

EXPERIMENTAL METHODS

A sketch of the experimental apparatus is shown in Figure 1. The apparatus consisted of five major components: boiler, plenum chamber, test tank, condenser and storage tank.

The vapor was generated in a cylindrical boiler 0.31 m in diameter and 0.46 m long. The boiler was equipped with a vacuum line for purging and removing dissolved gas from the system. The six immersion heating elements of the boiler had a diameter of 0.019 m and an active heating length of 0.27 m. The flow of vapor was controlled by adjusting the heater power with a Variac up to a maximum power of 4500 W.

During test operation, the vapor leaving the boiler passed through a line to the plenum chamber. The plenum chamber had a volume of 1.2×10^{-3} m^3, which was sufficient to eliminate pressure oscillations on the upstream side of the injector. Both the line from the boiler and the plenum chamber were heated to prevent vapor condensation.

The cylindrical test tank was 0.31 m in diameter and 0.76 m long. The volume of the test tank was sufficiently large to ensure relatively isothermal conditions during testing in spite of the energy release resulting from condensation of the vapor. The maximum bath temperature rise rate encountered during testing was 0.5 K/min.

Windows were provided in the test tank for lighting and observing the flow. An overflow system maintained a constant liquid head at the injector exit. The pressure in the bath was controlled by backfilling with argon through the pressure-vacuum line. The liquid temperature of the bath was controlled by heating tapes mounted on the walls of the test tank. Liquid temperatures were measured with several thermocouples spaced throughout the bath. The liquid temperature variation between thermocouples was less than 0.5 K, assuring uniform ambient bath conditions for the jet.

The condenser served as a vapor bypass when the system was brought to its operating condition as well as a sump for the overflow from the test tank during normal operation. The temperature of the condenser was controlled with a water cooling coil.

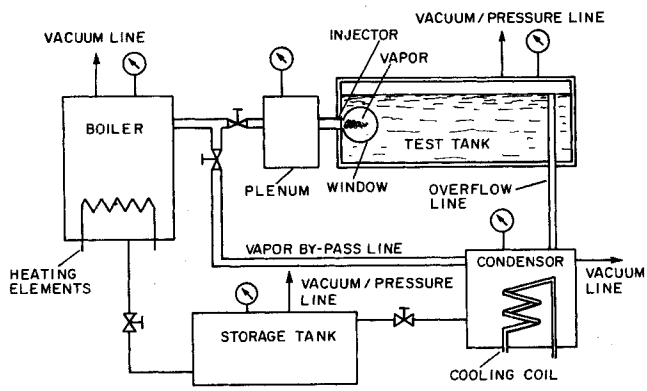

Fig. 1. Schematic diagram of the experimental apparatus.

The storage tank served as a sump for all the other tanks in the system as well as the source of liquid supply for the boiler. Liquid transfer to the boiler was accomplished by pressurizing the storage tank with argon.

The vapor injector was mounted flush with the end wall of the test tank. It consisted of a convergent nozzle with an exit diameter of 0.00317 m. A static pressure tap was located at the exit plane of the nozzle to ensure that the flow was choked at all test conditions. The jet flow was horizontal in order to eliminate hydrostatic pressure variations along the length of the vapor jet.

Pressures throughout the system were measured with absolute mercury manometers corrected for any liquid head in the lines. The line to the static pressure tap at the injector exit was kept purged of liquid by a small flow of argon.

The vapor jet was illuminated with a Strobotac having a flash duration of eight microseconds and photographed with a Graphlex camera. Six photographs were taken of the jet at each test condition in order to obtain an average vapor penetration length. The average picture-to-picture standard deviation of the penetration length was 8% (range 2 to 15%). As reported by Stanford and Webster (1972) and Kerney et al. (1972), it was necessary to thoroughly degas the liquid in the system prior to testing. In the absence of this precaution, a cloud of gas bubbles would eminate from the condensing jet, obscuring the photographs.

The materials employed in the tests were distilled water, ethylene glycol (Baker, analysed reagent), and iso-octane (Eastman Kodak, practical grade). The maximum temperature in the boiler was limited to 440 K for ethylene glycol and 395 K for iso-octane, in order to prevent decomposition of these liquids. The experimental data is listed in detail by Weimer (1972).

THEORY

The most complete previous attempt to analyze this process is the semi-empirical model of Kerney et al. (1972). In this earlier analysis, the condensation process was assumed to occur on an irregular gas-liquid interface separating a core flow of vapor from the surrounding liquid in the bath. The transport characteristics of the interface were treated by the assumption of a constant Stanton number. The Stanton number was evaluated empirically from penetration length data in a steam-water system at atmospheric pressure.

The model employed by Kerney et al. (1972) suffers from a number of fundamental defects and this approach was not continued in the present investigation. The major difficulty is that the earlier model is unable to suggest the influence of different liquid systems and bath pressures on the penetration length of the vapor in any fundamental manner. Furthermore, the assumption of a vapor core throughout the length of the two-phase portion of the jet

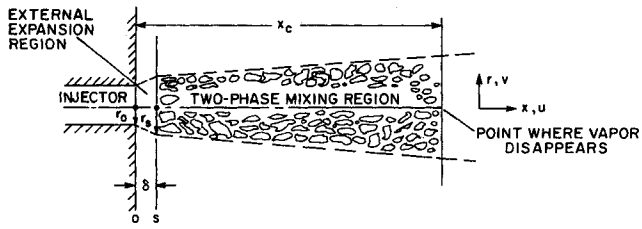

Fig. 2. Sketch of the theoretical model.

does not agree with other observations of turbulent gas injection into a liquid bath. For example, Liebson et al. (1956) indicate that a series of closely spaced irregular bubbles leave the injector exit for turbulent injector flow, as opposed to the presence of a gaseous cavity within an irregular boundary. Finally, the earlier model is clearly unsuitable for extension to long penetration lengths where individual bubbles are very evident in the flow.

In the present investigation, the condensing jet is treated as a two-phase, axisymmetric free jet with vapor bubbles and liquid dispersed throughout the jet. Analogous to the approach introduced by Bankoff (1960) for two-phase bubble flow in pipes, a variable density, single-fluid model was employed to represent the actual bubble-liquid mixture. This model implies that the local relative slip between the gas and liquid phases is zero at any point within the jet and that the major effect of the bubbles is to influence the density of the mixture. This approach seems plausible in the present case due to the small inertia of the bubbles, which suggests rapid equilibration of local liquid and vapor velocities within the jet boundaries.

Since many of the details of the present flow are unknown (distributions of velocity, void fraction, etc.), a very simplified model was considered for the turbulent mixing process. It was assumed that the distributions of velocity, etc., were similar at each axial location in the jet. In order to fix ideas, "top hat" profiles were employed for the mean flow quantities, that is, mean flow quantities are assumed to be constant over the pertinent diameter of the jet at each axial position [compare Equation (5)]. It is notable, however, that the general method is adaptable to other distribution functions when suitable information becomes available. The mixing process was treated through the use of a turbulent entrainment model for variable density jets first proposed by Morton (1965).

The external expansion of the vapor from conditions at the exit of the choked injector to the pressure of the bath presents an additional complication to the analysis of this process. In order to keep the model tractable, the external expansion of the vapor was assumed to occur in a distance much shorter than the penetration length of the vapor jet, and entrainment, frictional effects, and heat transfer were neglected for this process.

Following external expansion, the turbulent mixing of the jet was assumed to occur at constant pressure in the bath. This implies either horizontal injection with little turning of the jet due to buoyancy (as in the present tests) or small changes in hydrostatic pressure over the penetration length of the jet. In keeping with the lack of detail necessary for the bulk of the analysis, the decay of the potential core in the region near the injector exit was also ignored.

A sketch of the theoretical model is shown in Figure 2. Under the assumption of one-dimensional flow in the external expansion region, the absence of entrainment implies that the mass flow rate is constant in this zone. Therefore, the radius of the jet at the start of the mixing region is related to the injector exit radius through the equation of conservation of mass

$$r_s/r_0 = (G_0/G_s)^{1/2} \tag{1}$$

The injector exit mass velocity G_0 can be obtained directly from the mass flow rate and exit area of the injector. Neglecting losses in the external expansion region, the mass velocity at the start of the mixing region G_s was computed using the one dimensional conservation of energy equation, assuming an isentropic expansion between the injector exit conditions and the pressure of the bath.

The analysis of the mixing region is developed under the usual assumption for turbulent variable density jets. The flow is taken to be axisymmetric and the effects of molecular viscosity, and thermal conductivity are neglected in comparison to turbulent transport quantities. It is also assumed that $\overline{u'^2}$, $\overline{\rho' u'}$, $\overline{\rho' u'^2}$, etc., are small in comparison to the mean quantities u^2, ρu, ρu^2, etc. when integrated over the jet cross section. This imposes limitations on the magnitude of the turbulent fluctuations that may not be met in the present two-phase flow due to the possibility of large density fluctuations. However, this approximation is consistent with the method of Bankoff (1960), and there is little alternative in the absence of more detailed information on the turbulent structure of condensing jets.

Under these assumptions, the following equations for mean quantities may be obtained by integrating the equations of conservation of mass, momentum, and energy over the jet cross section

$$\frac{d}{dx}\int_0^\infty r\rho u dr = -(r\rho v)_{r=\infty} \tag{2}$$

$$\frac{d}{dx}\int_0^\infty r\rho u^2 dr = 0 \tag{3}$$

$$\frac{d}{dx}\int_0^\infty r\rho u(h - h_\infty) dr = 0 \tag{4}$$

In arriving at these equations, the mean axial velocity component and all turbulent fluctuation terms have been taken to be zero at large distances from the axis of the flow. The integration constant on the right-hand side of Equation (2) represents the entrainment of the ambient fluid by the jet.

The following top hat profiles were assumed for the mean flow quantities.

$$u(x,r) = \begin{cases} u(x) & 0 \le r \le a(x) \\ 0 & a(x) < r \end{cases}$$

$$\rho(x,r) = \begin{cases} \rho(x) & 0 \le r \le \lambda a(x) \\ \rho_\infty & \lambda a(x) < r \end{cases} \tag{5}$$

$$h(x,r) = \begin{cases} h(x) & 0 \le r \le \lambda' a(x) \\ h_\infty & \lambda' a(x) < r \end{cases}$$

In Equations (5), $a(x)$ is the local radial length scale characterizing the velocity distribution. As in other turbulent jet studies, λ and λ' are assumed to be constant scalar factors representing the different radial length scales pertinent to the density and enthalpy profiles. Studies of single phase turbulent free jets in liquids and gases have shown that the spread of thermal energy and matter is generally more rapid than the spread of velocity (Hinze,

1959). For the condensing jet in water, Kerney (1970) also observed that the liquid temperature distribution was broader than the velocity distribution in the region downstream of the point where condensation is complete (unfortunately, measurements were not made in the two-phase region which is more pertinent to the present analysis). Based on this evidence, λ and λ' were assumed to be greater than unity in the present analysis.

The following expression was employed for the rate of entrainment of mass by the jet.

$$-(r\rho v)_{r=\infty} = \rho_\infty E_0 au(\rho/\rho_\infty)^{1/2} \tag{6}$$

This equation was suggested by Morton (1965) for turbulent jets or plumes having a density different than the ambient fluid. The square root density ratio results from measurements of the rate of entrainment of various gas jets in still air ($0.66 < \rho_\infty/\rho_s < 14.5$) by Ricou and Spalding (1961). The quantity E_0 is the entrainment constant of the jet. Ricou and Spalding (1961) found an entrainment constant of 0.08 in their investigation, with values of this parameter in the range 0.06 to 0.12 resulting from earlier work on fully developed isothermal air jets.

With the entrainment law given by Equation (6), the equations of motion can be reduced to a form identical to that of incompressible jets by introducing a new radial scale factor (Morton, 1965).

$$b(x) = (\rho/\rho_\infty)^{1/2} a(x) \tag{7}$$

Substituting Equations (5) to (7) into Equations (2) to (4), integrating and simplifying yields the following equations for the flow.

$$\frac{d}{dx}(ub^2) = 2E_0 ub \tag{8}$$

$$\frac{d}{dx}(u^2b^2) = 0 \tag{9}$$

$$\frac{d}{dx}[ub^2(h - h_\infty)] = 0 \tag{10}$$

Neglecting the external expansion length δ, the initial conditions for Equations (8) to (10) are

$$x = 0; \quad \rho = \rho_s, \quad u = u_s, \quad h = h_s, \quad a = r_s \tag{11}$$

Equation (7) gives the corresponding initial value of b as follows:

$$x = 0; \quad b = (\rho_s/\rho_\infty)^{1/2} r_s \tag{12}$$

Integrating Equations (8) to (10), subject to the boundary conditions of Equations (11) and (12), yields the following solution for the flow.

$$\frac{h_s - h_\infty}{h - h_\infty} = \frac{u_s}{u} = \frac{b}{r_s}\left(\frac{\rho_\infty}{\rho_s}\right)^{1/2} = 1 + 2E_0\left(\frac{\rho_\infty}{\rho_s}\right)^{1/2}\frac{x}{r_s} \tag{13}$$

Equation (13) implies that the jet will more rapidly approach ambient conditions as the value of ρ_∞/ρ_s increases. Physically, this reflects the reduced inertial and thermal capacity of a jet having a density much lower than the ambient fluid.

In order to associate the results of Equation (13) with the penetration length of the vapor, it is necessary to introduce the equation of state of the liquid-vapor mixture. In this regard, the condition of local thermodynamic equilibrium is imposed in addition to the assumption of intimate mixing between the liquid and vapor phases within the jet boundary.

The most general situation involves a superheated vapor at the start of the mixing region. In this case, the model implies that the liquid entrained by the jet would become vaporized until the enthalpy of the jet reaches the saturated vapor enthalpy appropriate to the local bath pressure. As the mean enthalpy of the jet decreases through mixing in this zone, the temperature of the jet decreases. When the temperature of the jet reaches the saturation temperature (for the local bath pressure) liquid must begin to appear within the jet for thermodynamic equilibrium to be maintained. In this second region, the two phases within the jet are at the saturated liquid and vapor states, respectively, and the reductions in the mean jet enthalpy through mixing are reflected by a reduction in the mean quality of the jet (while the temperature of the jet remains at the saturation temperature). The mean jet quality at any point in this region is related to the mean jet enthalpy as follows:

$$Y = (h - h_f)/h_{fg} \tag{14}$$

Once the enthalpy of the jet reaches the saturated liquid enthalpy, the mean quality is zero. Beyond this point, the temperature of the jet falls, much as in the superheated region, as the mean enthalpy continues to decrease through mixing.

Within the context of a uniformly mixed jet with top hat profiles, the condensation process is completed when the enthalpy of the jet is equal to the saturated liquid enthalpy. Formally, this implies that the vapor penetration length could be determined by setting $h = h_f$ in Equation (13) and solving for the distance x. However, h represents an average value over the jet and higher values will be present along the centerline at any axial position. Since a local enthalpy greater than h_f, at any radial location, will still cause vapor to be observed in the experiments, the end of condensation will not really be reached until the enthalpy is less than h_f at all radial positions. In the self preserving region of single-phase jets, the ratio of the average to the maximum value (at the centerline) of any normalized quantity is a fixed fraction, for example,

$$(h - h_\infty)/(h - h_\infty)_{\max} = \epsilon \tag{15}$$

In the case of Gaussian profiles with a scale factor of unity, Murgai and Emmons (1960) show that $\epsilon = 1/2$. Since varying functional forms and scale factors for the profiles yield different values for ϵ, this quantity will be left as an empirical constant for the present two-phase flow.

Setting $(h - h_\infty)_{\max} = (h_f - h_\infty)$ in Equation (15) and combining this result with Equations (1) and (13) yields the following expression for the vapor penetration length

$$x_c/r_0 = (G_0/G_s)^{1/2}[1 + (1 - \epsilon)B]/[2\epsilon E_0(\rho_\infty/\rho_s)^{1/2} B] \tag{16}$$

The quantity B represents the driving potential for the condensation process, defined as follows:

$$B = (h_f - h_\infty)/(h_s - h_f) \tag{17}$$

For low values of B, representative of the bulk of existing test data on vapor penetration lengths, Equation (16) assumes the following asymptotic form.

$$x_c/r_0 = (G_0/G_s)^{1/2}/[2\epsilon E_0(\rho_\infty/\rho_s)^{1/2} B] \tag{18}$$

The present driving potential for condensation is somewhat more generalized than the driving potential defined as follows by Kerney et al. (1972).

$$B = c_p(T_f - T_\infty)/h_{fg} \tag{19}$$

TABLE 1. RANGE OF TEST VARIABLES

Quantity	Ethylene glycol	Iso-octane	Water	Water (Kerney, et al. 1972)	Water (Stanford, & Webster, 1972)
Number of tests	121	18	150	129	8
Injector diam., m	0.00317[a]	0.00317[a]	0.00317[a]	0.004-0095[b]	0.0109-0.0172[c]
B	0.0088-0.20	0.068-0.30	0.0025-0.063	0.032-0.15	0.11-0.14[d]
ρ_∞/ρ_s	3260-31200	324-1180	3980-27700	1430-1635	1600
G_0/G_s	1.59-7.62	1.05-1.93	1.17-4.13	1.01-3.06	1.05-1.75
Prandtl number[e]	17-41	4.2-4.5	2.6-5.5	1.9-2.7	2.7-2.9[d]
Reynolds number[f]	1.5-6.3 $\times 10^4$	1.5-2.2 $\times 10^5$	2.2-4.4 $\times 10^4$	2-150 $\times 10^4$	2.8-6.2 $\times 10^5$
Bath pressure (N/m^2)	1.4-19 $\times 10^3$	15-58 $\times 10^3$	4.6-38 $\times 10^3$	1.013 $\times 10^5$	1.013 $\times 10^5$

[a] Flush mounted wall injector.
[b] Flush mounted and conical injectors.
[c] Tube injectors.
[d] Range results from uncertainty in bath temperature.
[e] At arithmetic average of bath and saturation temperature.
[f] At injector exit conditions.

Equation (17) only reduces to Equation (19) when the jet is a saturated vapor at the start of the mixing process and the liquid specific heat is a constant.

Equations (16) to (18) comprise the fundamental relations for correlating the penetration length of the vapor. The major assumptions employed in arriving at these equations were axisymmetric flow, short external expansion region with negligible entrainment and losses, a single fluid model of the two-phase flow, entrainment given by the Morton entrainment law, and molecular transport small in comparison to turbulent effects. Properties at the start of the mixing process, state(s), are computed by assuming an isentropic expansion from the injector exit conditions. The quantities ϵ and E_0 were treated as empirical constants to be determined by correlating experimental data. Earlier work suggests that ϵ is on the order of ½ (Murgai and Emmons, 1960) and E_0 is in the range 0.06 to 0.12 (Ricou and Spalding, 1961), however, these earlier determinations involved single-phase flows having density ratios far smaller than those encountered in the present investigation.

RESULTS AND DISCUSSION

The experimental results from both Kerney et al. (1972) and the present investigation were employed in seeking correlations for the vapor penetration length. The overall test range of these experiments is summarized in Table 1.

Since B is much smaller than unity for the available experimental results, the asymptotic form of the theoretical penetration length expression [Equation (18)] was employed during initial correlation attempts. Fitting the data to Equation (18) yielded the following expression

$$x_c/r_0 = 35.5\ (G_0/G_s)^{1/2}/[(\rho_\infty/\rho_s)^{1/2}\ B] \qquad (20)$$

Figure 3 shows the comparison between Equation (20) and the experimental data. The data of Kerney, et al. (1972) is represented by a least squares curve in order to reduce cluttering of the figure. (It is notable that the slope of this least squares curve was found to be 0.998, which is very close to the theoretical value of unity.) The average of the absolute deviation of the experimental penetration lengths from the values given by Equation (20) is 21.9%. The data used in developing Equation (20) is limited to choked injector flows with dimensionless penetration lengths in the range 3 to 70. Unchoked flow in the injector causes an unstable oscillatory behavior of the jet which invalidates the correlation (Kerney, et al. 1972). Data for penetration lengths greater than 70 was excluded due to buoyancy effects which were indicated by the upward turning of the tip of the horizontal vapor jet. Penetration lengths shorter than 3 were not considered due to the difficulties of accurate measurement and the complications of developing flow and the external expansion process near the injector exit.

A portion of the data obtained by Stanford and Webster (1972), which satisfies the above criteria, is also shown in Figure 3. The specific range of these tests is summarized in Table 1. For some of these tests the bath temperature was only stated to lie in the range 297 to 311°K which results in an uncertainty in the value of B through Equation (17). The range of the data points influenced by this uncertainty is indicated in Figure 3. Stanford and Webster (1972) also did not explicitly measure conditions at the exit of the injector. Therefore, it was necessary to assume that the steam left the injector as a saturated vapor in order to compute the abscissa of the plot for this data. While the error introduced by this assumption is of uncertain magnitude; based on the experience of the present test program it is not likely to be greater than 10%. The agreement of the measurements of Stanford and Webster (1972) with the other results is not good at the shorter penetration lengths but appears to be improving as the value of the abscissa increases.

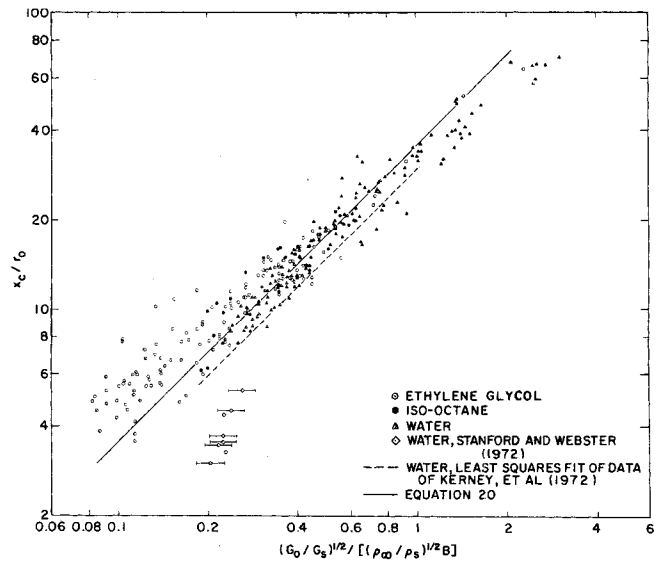

Fig. 3. Experimental dimensionless vapor penetration lengths.

For the present test results, Figure 3, the three liquids give about the same results in spite of a rather large variation of Prandtl number (Table 1). This suggests that the flow is relatively insensitive to molecular transport properties, a result quite typical of highly turbulent jets (Hinze, 1959).

Comparing Equations (18) and (20) indicates that the product $\epsilon E_0 = 0.0141$, for the present condensing jet experiments. This yields a value of ϵ in the range 0.12 to 0.24, if the entrainment constant is taken to lie in the range 0.06 to 0.12 (Ricou and Spalding, 1972). This range of ϵ is somewhat lower than the value $\epsilon = \frac{1}{2}$, appropriate for Gaussian profiles with unity scale factors (Murgai and Emmons, 1960). However, in view of the two-phase nature and much higher density ratios of the present jets in comparison to the test conditions of Ricou and Spalding (1961), agreement to this degree is reasonably satisfying. This finding suggests that condensing jets exhibit gross similarities to the transport and mixing characteristics of conventional single phase jets when allowance is made for the large density variation of condensing jets.

A second correlation attempt was based on the use of Equation (16), as opposed to the asymptotic form of Equation (18). Least squares fitting of the data gave the following expression in this case:

$$x_c/r_0 = 30.9\ (G_0/G_s)^{1/2}(1 + 2.25B)/[(\rho_\infty/\rho_s)^{1/2}\ B] \quad (21)$$

This equation gave an average absolute deviation between the measured and predicted values of the penetration length of 20.5%, providing little improvement in accuracy over Equation (20). The standard deviation of the constant 2.25 in Equation (21) was 0.30. The value of this constant implies a negative value of ϵ, through Equation (16), which is meaningless. This behavior is probably due to the fact that this term becomes important for large values of B where the penetration length is short. Under these conditions, the jet is influenced by external expansion and flow development effects which are not included in the present analysis. Apparently, these latter effects are of sufficient magnitude to override the formal dependence on ϵ, suggested by Equation (16), at large B values.

An improved data correlation can be obtained by removing the theoretical restrictions on property powers prior to least squares fitting. Assuming a power relationship between B, ρ_∞/ρ_s, G_0/G_s and x_c/r_0 yields the following equation:

$$x_c/r_0 = 20.57\ (G_0/G_s)^{0.713}/[(\rho_\infty/\rho_s)^{0.384}\ B^{0.801}] \quad (22)$$

Equation (22) had a multiple correlation coefficient of 0.957 with an average absolute deviation between the measured and predicted values of penetration length of 13.0%. In Equation (22), the standard deviations of the powers of B, ρ_∞/ρ_s and G_0/G_s were 0.012, 0.012 and 0.029 respectively. Including additional parameters such as injector Reynolds number and the liquid Prandtl number resulted in only a minor increase in the accuracy of the correlation.

The above findings indicate that the turbulent condensing jet flowing from a choked injector is in many ways similar to a turbulent single phase jet. As in the case of turbulent single phase jets, the mixing characteristics of the condensing jet appear to be relatively independent of molecular Prandtl number and injector Reynolds number (over the range indicated in Table 1). The product ϵE_0 is also of the same order of magnitude for both condensing and single phase jets, when allowance is made for the large density variations of the condensing jets. However, detailed measurements of the structure of the condensing jet (distribution of void fraction, velocity, etc.) would be desirable in order to completely evaluate the similarities between the two cases.

The parameters in the present correlation suggest the possibility of application to reacting or dissolving jets, by analogy, through a proper redefinition of the driving potential B. However, the accuracy and limitations of such a procedure remain to be tested (in particular, varying scale factors for different mean flow quantities would suggest changes in the constant in Equation (20)). Further investigation of flow development and buoyancy effects on the condensing jet, as well as unchoked injector operation, would also be desirable.

ACKNOWLEDGMENTS

This work was supported by the Ordnance Research Laboratory of The Pennsylvania State University under contract with the Naval Ordnance Systems Command. The assistance of J. F. Avery with portions of the experimental program is also gratefully acknowledged.

NOTATION

a = radial length scale, m
b = reduced radial length scale, Equation (7), m
B = driving potential for condensation, Equation (17)
c_p = liquid specific heat, J/kg·K
E_0 = entrainment constant, Equation (6)
G = mass velocity, kg/m²·s
h = enthalpy, J/kg
h_{fg} = enthalpy of vaporization, J/kg
r = radial distance, m
T = temperature, K
u, u' = mean and fluctuating axial velocity, m/s
v = mean and fluctuating radial velocity, m/s
x = axial distance, m
Y = quality of the jet, Equation (14)
δ = length of external expansion region, m
ϵ = profile factor, Equation (15)
λ, λ' = ratio of length scales of density and enthalpy profiles to that of the velocity profile
ρ, ρ' = mean and fluctuating density, kg/m³

Subscripts

c designates point where condensation is complete
f designates saturated liquid state at the bath pressure
s designates conditions at the completion of external expansion
0 designates injector exit condition
∞ designates conditions in the ambient bath

LITERATURE CITED

Bankoff, S. G., "A Variable Density Single-Fluid Model for Two Phase Flow with Particular Reference to Steam-Water Flow," Trans. ASME, *J. Heat Transfer*, 265 (1960).

Gilbert, W. D., and D. Bozic, "The Analysis of Two Phase Flow in a Jet," *Trans. Eng. Inst. Can.*, 9, 1 (1966).

Glikman, B. F., "Experimental Research of the Stream of Steam in a Space Filled Out by a Liquid," Rept. of Academy Sci. U.S.S.R., Div. Techn. Sci., Energetics Autom., 1, 39 (1959).

Hinze, J. O., *Turbulence*, pp. 420-431, McGraw-Hill, New York (1959).

Kerney, P. J., "Characteristics of a Submerged Steam Jet," Ph.D. thesis, Penn. State Univ., University Park (1970).

———., G. M. Faeth, and D. R. Olson, "Penetration Characteristics of a Submerged Steam Jet," *AIChE J.*, 18, 548 (1972).

Liebson, I., E. G. Holcomb, A. G. Cacoso, and J. J. Jacmic, "Rate of Flow and Mechanics of Bubble Formation from Single Submerged Orifices," *ibid.*, **2**, 296 (1956).
Morton, B. R., "Modeling Fire Plumes," Tenth Symp. (Intern.) on Combustion, pp. 973-982, The Combustion Institute, Pittsburgh, Pa., (1965).
Murgai, M. P., and H. W. Emmons, "Natural Convection Above Fires," *J. Fluid Mech.*, **8**, 611 (1960).
Ricou, F. P., and D. B. Spalding, "Measurements of Entrainment of Axisymmetrical Turbulent Jets," *ibid.*, **11**, 21 (1961).
Stanford, L. E., and C. C. Webster, "Energy Suppression and Fission Product Transport in Pressure-Suppression Pools," Oak Ridge Nat. Lab. Report, ORNL-TM-3448 (1972).
Weimer, J. C., M.S. thesis, Penn. State Univ, University Park (1972).

Manuscript received September 11, 1972; revision received December 8, 1972; paper accepted December 11, 1972.

Photopolymerization of Acrylamide in an Annular Flow Reactor

Rates of homogeneous polymerization of aqueous solutions of acrylamide were measured in an annular flow reactor at 35°C. By independent determinations of the quantum yield for the initiation step and the light intensity, it was possible to identify reaction orders and to calculate ratios of rate constants for the polymerization process.

An empirical kinetics model, based upon producing activated molecules solely from initiator ($K_2S_2O_8$), best fit the data. According to this model the rate is 3/2 order in monomer concentration, 1/2 order in initiator, and proportional to the 1/2 power of the intensity of absorbed radiation. The effect of monomer concentration on the induction period and the 3/2 order with respect to monomer indicate a complex initiation process.

DAN SANDRU
and
J. M. SMITH

Department of Chemical Engineering
University of California
Davis, California

SCOPE

Kinetic studies of homogeneous photopolymerization in batch systems have a long history (Bagdasar'yan, 1968, 1944, 1947, 1948, 1949; Bamford, 1949; Bevington, 1961; Flory, 1953; Hamm, 1967; Huysor, 1970; Mark and Raff, 1961; Marvel and Levesque, 1939; Marvell and Riddle, 1940; Newkirk, 1946; Taylor and Vernon, 1930). The objectives in these investigations were to determine the effect of concentrations and light intensity on the rate. Only rarely were numerical values obtained for the kinetic constants. From an applied viewpoint it is important to be able to use kinetic data to predict the performance of continuous flow reactors. For this purpose it is necessary to have a numerical rate equation and also a design procedure to account for the variations in rate with location in the reactor. This engineering aspect of photopolymerization has not been treated in the literature to our knowledge, except in a recent work by Jain, Graessley, and Dranoff (1970) on styrene polymerization in dilute solutions.

The objective of this work was to measure rates quantitatively for a typical system—the polymerization of acrylamide in an annular flow differential reactor. Acrylamide was chosen since it represents a typical monomer which forms water-soluble polymer and since some numerical rate information obtained in a batch system (Suen et al., 1958) is available. The data were used to test models for the kinetics of the polymerization process, particularly to determine the order of the rate with respect to monomer and initiator concentrations and with respect to light intensity.

CONCLUSIONS AND SIGNIFICANCE

The practicality of an experimental method for measuring photopolymerization rates in a flow reactor has been demonstrated by studying the homogeneous polymerization of acrylamide with a polychromatic radiation source. It was shown that the quantum yield for the initiation step can be estimated by first operating the annular reactor as a batch-recycle unit during the induction period. In the subsequent part of a run, operation was changed to a once-through differential basis for which rates of polymerization could be measured.

It was shown further that the rate data, combined with independent measurements of light intensity and of quantum yield for the initiation step, could be used to evaluate various models of polymerization kinetics. In particular the order of the overall reaction with respect to concentrations and light intensity could be established. For our acrylamide study the 1.5 order for monomer concentration indicated an interaction effect, such as complex formation, or cage effect, between monomer and activated initiator molecules. Also numerical values of rate-constant ratios could be evaluated based upon certain assumptions, par-